2023 62nd IEEE Conference on Decision and Control (CDC)
December 13-15, 2023. Marina Bay Sands, Singapore

Distributed Feedforward Optimization for Control of Multi-Energy Network with Temporal Variations

Yiqiao Xu, Zhengfa Zhang, Zhengtao Ding, Shuoying Jiang, and Alessandra Parisio

Abstract— **Multi-Energy Network (MEN) is a promising approach to improve the overall efficiency of energy utilization. Yet, balancing its electrical and thermal power in real-time is challenging due to variable demands. In this paper, we formulate a distributed Time Varying Optimization Problem (TVOP) and solve it in continuous-time to track the unknown time-varying optimal trajectories. First, we apply the principles of output regulation theory to reverse engineer the feedforward laws in the presence of projection. These laws are responsible for proactively canceling the effects of temporal demand variations. Then, a projection-based distributed optimization algorithm, alongside a distributed auxiliary protocol based on weighted-sum consensus, result in a novel scheme we term distributed feedforward optimization. One of the key features of our scheme is its data-driven nature, where temporal variations are captured from Ultra-Short-Term Forecasting (USTF) profiles using an exosystem. Under mild assumptions, the proposed scheme provides a guarantee for asymptotic convergence. Simulation results demonstrate the effectiveness of our scheme under an non-ideal case.**

I. Introduction

As the world moves towards a Net Zero future, reconciling the growing demand for energy with the need to reduce carbon emissions has become an imperative [1]. The Multi-Energy Network (MEN) plays a crucial role as it enables the integration of different power sectors, such as electrical and thermal, to improve energy efficiency [2]. Recently, the Fifth-Generation District Heating and Cooling (5GDHC) networks have received significant interest [3]. Compared with traditional heating networks, 5GDHC network operates at a low temperature range of 10–25°C, resulting in lower heat losses. It also offers bidirectional operation to meet both heating and cooling demands simultaneously.

Given the coupling between different energy sectors, MEN control is a complex task. The authors in [4] proposed an agent-based control for a low-temperature network. In [5], the authors offer an integrated approach for optimal operation of MEN and thermal comfort management in buildings. These studies did not feature dynamics and exhibit deficiency in the predictive capability, which is a necessity for optimal operation. Among several optimization-based methods, Model Predictive Control (MPC) is known to be promising for power and energy applications and have satisfying performance when the system dynamics are well captured and the model is accurate. A centralized MPC scheme was proposed in [6] for energy management of a 5GDHC-based MEN. However, the difficulty in modeling is compounded by MENs, which may have numerous interconnected subsystems with nonlinear dynamics. Furthermore, centralized approaches are computationally prohibitive for such complex and large systems.

Optimal Resource Allocation (ORA) involves optimizing the allocation of a limited set of resources to minimize some convex cost function. By formulating the control problem as an optimization problem, it serves as an alternative to achieve the control goal while being model-free. Effective methods to solve it employ a dynamical system to approach the optimal solution in continuous time [7]. These methods demonstrate their limitations when dealing with more complex Time-Varying Optimization Problems (TVOPs). Such limitations may lead to the emergence of an optimality gap, the extent of which depends temporal variations including time-varying cost functions and constraints. As the optimality gap persists, the dynamical system may struggle to adapt to changing conditions and maintain efficient resource utilization. While distributed algorithms for time-invariant problems have been well established, there are few works targeting TVOPs, and even fewer distributed TVOPs. Some preliminary results for unconstrained and constrained TVOPs can be found in [8]–[10]. However, achieving vanishing tracking errors in a distributed manner is not trivial. Schemes without predictive capability would render a uniformly ultimately bounded optimality gap [9]. For centralized TVOPs, the tracking error can be accurately eliminated by using a prediction-correction scheme [10], [11], but it is no longer true for distributed TVOPs [12]. The Hessian matrix needs to be aggregated via a finite-time or fixed-time consensus protocol [13]–[15]; otherwise access to this global information is needed. Similarly, a distributed estimator based on fixed-time consensus is developed in [16] to predict the time derivative of the optimal trajectory.

None of these works have explored the feasibility of canceling the effects of temporal variations via a feedforward design. Recently, in [17], the author applies the principles of output regulation theory to transform distributed TVOPs into time-invariant ones, simplifying the derivations considerably. Thus, this paper builds upon the findings in [7], [17] to develop a more effective scheme for solving distributed TVOPs, along with extensions suitable for use in MENs. With a feedforward design, the use of finite-time or fixed-time consensus is no longer a prerequisite to solving distributed TVOPs. The resulting control scheme, named as distributed feedforward optimization, is fully distributed

This work was partially supported by Supergen Energy Networks Hub (EP/S00078X/2), Multi-energy Control of Cyber-Physical Urban Energy Systems (EP/T021969/1), and Grid Scale Thermal and Thermo-Chemical Electricity Storage (EP/W027860/1). The authors are with the Department of Electrical and Electronic Engineering, The University of Manchester, U.K. (emails: yiqiao.xu; alessandra.parisio@manchester.ac.uk)

and allows for predictive capability to cancel the impacts of temporal variations. The main contribution of this paper lies in a better handling of local feasibility constraints, for which the reverse engineering methodology, distributed auxiliary protocol, and distributed optimization algorithm are re-established based on projection. It is worth noting that local feasibility constraints are disregarded by [13]–[17], despite their significant relevance in practical applications. Furthermore, we extend the feedforward design to a more general form to accommodate time-varying affine equality constraints related to MENs. However, the explicit wave format of those constraints is not a reasonable assumption for MENs. As advanced forecasting tools [18] have become available, we propose to capture the temporal variations from Ultra-Short-Term Forecasting (USTF) profiles, which yield a time window of a few minutes to up to 1 hour ahead and a time resolution ranging from seconds to minutes [19]. Thus, the proposed scheme holds a data-driven feature.

II. Preliminaries

A representative MEN consists of a central plant, a circulation pump, nodes, electrical lines, and water pipes [20]. In this paper, the electrical network under consideration is an islanded low-voltage sub-network that represents an urban district. As this has been extensively modeled in the literature, e.g., [21], in the following we will concentrate on the thermal aspects.

The concept of 5GDHC network is necessarily linked to the use of Water-Source Heat Pumps (WSHPs) for climatization. The central plant is only responsible for maintaining the temperature at return/supply pipes within a certain range. The circulation pump provides pressure to ensure necessary mass flows inside. It is assumed that the central plant and circulation pump, and WHPs are controlled separately.

A. Pipe

In water pipelines, the mass flow goes slowly from the inlet to the outlet. During this process, there is heat exchange with the surroundings. Thus, a frequency domain representation for real-time water temperature at the outlet of a pipe is given by [22]

$$T_{out}(s) = \left[(T_{in} - T_a)\, e^{-\frac{\lambda_p L}{c_w \dot{m}}} + T_a \right] e^{-\tau s}, \tag{1}$$

where T_{in} represents the inlet temperature, T_a denotes the ambient temperature, $\dot{m}$ is the mass flow rate through the pipe, c_w represents the specific heat capacity of water, L is the length of the pipe, and λ_p is the heat transfer coefficient determined by the material and manufacture. By linearizing the fluid mechanical equations, we can simplify the transport phenomena into a time delay denoted by τ between the inlet and outlet [23]

$$\tau = \rho_w \pi D^2 L / \left(4\dot{m}\right), \tag{2}$$

where D represents the diameter of the pipe and ρ_w is the density of water.

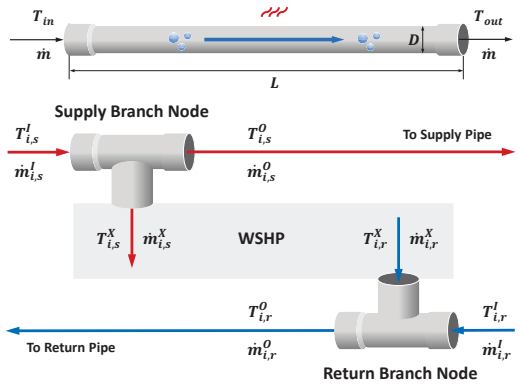

Fig. 1. Schematic illustration of pipes and nodes in 5GDHC network.

B. Node

Thermally, a load bus node can be subdivided into a supply branch node, a return branch node, and a WSHP. Here, water mass flow in the supply branch is diverted here, and a portion of the water is exported to the WSHP and finally the return branch, while the other remains along the trunk pipe. A schematic illustration is provided in Fig. 1.

The mass flow rates at the supply/return branch nodes for $i \in \mathcal{L}$ satisfy [24]

$$\dot{m}^I_{i,s} = \dot{m}^X_{i,s} + \dot{m}^O_{i,s}, \tag{3}$$
$$\dot{m}^O_{i,r} = \dot{m}^X_{i,r} + \dot{m}^I_{i,r}, \tag{4}$$

where the subscripts s and r correspond to the supply and return branches while the superscripts I, O, and X correspond to the input, output, export ports, respectively.

For supply branch node, we have

$$T^I_{i,s} = T^X_{i,s} = T^O_{i,s}, \tag{5}$$

whereas the mass flows into the return branch node are mixed, resulting in a temperature that can be calculated by

$$T^O_{i,r} = \left(\dot{m}^I_{i,r} T^I_{i,r} + \dot{m}^X_{i,r} T^X_{i,r}\right) / \dot{m}^O_{i,r}. \tag{6}$$

C. WSHP

Through a small amount of high electrical energy input, WSHP achieves the transfer of heat between water sources. Coefficient of Performance (COP) and Energy Efficiency Ratio (EER) evaluate the heating and cooling performance. Their relation to $T^X_{i,s}$ and $T_{i,u}$ can be described using a performance map [20]

$$COP_i \text{ or } EER_i = \mathcal{F}(T^X_{i,s}, T_{i,u}), \tag{7}$$

where $T_{i,u}$ is a temperature set by user.

This paper considers winter scenarios where only heating is required. The electrical power $P_{i,HP}$ and heat exchange $\dot{Q}_{i,ex}$ of WSHP can be expressed by

$$P_{i,HP} = \dot{Q}_{i,HP} / COP_i, \tag{8}$$
$$\dot{Q}_{i,ex} = \dot{Q}_{i,HP} - P_{i,HP}, \tag{9}$$

where $\dot{Q}_{i,HP}$ is the thermal power injected by WSHP. The mass flow rate through the WSHP is adjusted according to

$$\dot{m}^X_{i,s/r} = \dot{Q}_{i,ex} / \left(c_w \Delta T\right), \tag{10}$$

where ΔT is the temperature drop between $T^X_{i,s}$ and $T^X_{i,r}$ that has a default setting of 5 °C [20].

Due to slight fluctuations in supply water temperature at the central plant, as well as factors like heat exchange for climatization and heat loss during water transport, the COPs of all WSHPs will exhibit fluctuations throughout network operation. It is necessary to account for the dynamics in (1)–(10) in the optimization problem. This will be elaborated in Section III.

III. Problem Formulation

Because of the presence of droop controllers and damping components, any electrical power imbalance will induce a scaled deviation in the synchronous frequency [21]. Thus, along the operation, the power set points for DG inverters and WSHPs, expressed in $x_i, \forall i$, should adhere to the following constraint to restore frequency:

$$\sum_{i\in\mathcal{G}} x_i - \sum_{i\in\mathcal{L}} x_i = \sum_{i\in\mathcal{L}} P_{i,L}(t), \tag{11}$$

where we introduce $\mathcal{G}$ as the set of Distributed Generation (DG) nodes and $\mathcal{L}$ the set of load bus nodes; for $i \in \mathcal{L}$, each node is equipped with a WSHP; $P_{i,L}(t)$ is the time-varying electrical power demand for node i.

A MEN can be partitioned into multiple thermal zones according to building clustering and storage infrastructure [25], with each zone served by at least one WSHP. For thermal comfort of the occupants, WSHPs are asked to provide thermal power as requested, which yields an additional equality constraint for each thermal zone:

$$\sum_{i\in\mathcal{Z}_k} \mathcal{F}(T^X_{i,s}, T_{i,u}) \cdot x_i = \dot{Q}_{k,L}(t), \tag{12}$$

where $\mathcal{Z}_k$ represents the set of thermal zones and $\dot{Q}_{k,L}(t)$ is the time-varying thermal power demand for thermal zone k.

Consider n nodes and z zones. Minimizing the overall operational costs $\sum_{i=1}^n f_i(\cdot)$ over $x_i \in \mathcal{X}_i, \forall i$ with respect to (11)–(12) will lead to

$$\underset{x_i\in\mathcal{X}_i,\forall i}{\text{Minimize}} \quad \sum_{i=1}^n f_i(x_i), \tag{13a}$$

$$\text{Subject to} \quad Ax = Bd(t) \text{ and } (1)\text{–}(10), \tag{13b}$$

where $A \in \mathbb{R}^{(1+z)\times n}$, $B \in \mathbb{R}^{(1+z)\times(n+z)}$, $x \in \mathbb{R}^n$, and $d(t) \in \mathbb{R}^{n+z}$ is a vector of $P_L(t)$ and $\dot{Q}_L(t)$. Usually, $d(t)$ is measurable or can be estimated in real-time [26].

Remark 1: Problem (13) is a distributed TVOP in which the equality constraint varies with time, setting it apart from time-invariant problems as considered in the literature. There are of course cases where the cost functions are also time-varying, such as real-time electricity price. However, this is not pertinent to the ultra-short-term time window under consideration, and any variation in price is likely to be negligible. Actually our proposed scheme can easily be modified to deal with time-varying cost functions. Furthermore, we would like to emphasize that matrix A in equation (13b) can be unequivocally regarded as time-invariant, as the dependence of COP_i for all i on the time-domain is only indirect, via the dynamics outlined in (1)–(10).

IV. Main Results

As relying solely on measurements would result in a passive situation, we propose to incorporate prior information to allow for predictive capability that is key for tracking.

A. Capturing Temporal Variations

In output regulation theory, an exogenous signal is an external input that affects the operation of the system but is not manipulated by the system. This is analogous to the temporal variation discussed in this paper. It was proved that an internal model of the exogenous signals can be effectively used in the design of output regulators [27], where the concept of exosystem plays a key role.

A neutrally stable linear exosystem of the sinusoidal form is as follows:

$$\dot{v}(t) = Sv(t), \tag{14}$$

with $v(t) \in \mathbb{R}^{2N}$ being a function of time

$$v(t) = \left[\cos(\omega_0 t), \sin(\omega_0 t), \cdots, \cos(N\omega_0 t), \sin(N\omega_0 t)\right]^\top,$$

where $S \in \mathbb{R}^{2N\times 2N}$, N is the number of sines (or cosines), and ω_0 is the fundamental frequency to select.

In the context of MEN, it is more realistic to think that we do not exactly know the temporal variations, which need to be captured from USTF profiles. Here a combination of N sines and N cosines is employed for fitting:

$$r_i(t) = \sum_{k=1}^N a_{ik}\cos(k\omega_0 t) + \sum_{k=1}^N b_{ik}\sin(k\omega_0 t), \tag{15}$$

where $r_i(t)$ is the temporal demand variation, and a_{ik} and b_{ik} are fitting coefficients. As such, the temporal variation can be replicated as an affine mapping of the exosystem output, as illustrated in Fig. 2. Considering the real-world error between what we captured and measured, $d_i(t)$ in (13b) becomes

$$d_i(t) = r_i(v) + e_i, \tag{16}$$

where e_i can arise from both forecasting and fitting.

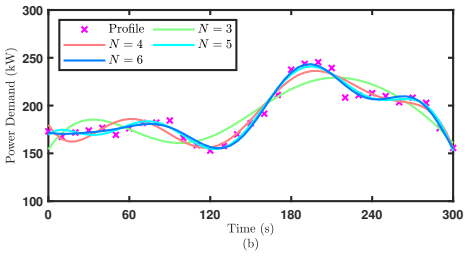

Fig. 2. Temporal variations within a USTF profile, captured by exosystems of different orders and provided 5-min ahead of time.

B. Reverse Engineering

Next, we are going to reverse engineer how the optimal trajectories look like when the local feasibility constraints are handled by projection. Denote the optimal trajectory of node i for Problem (13) by $\pi_i(v) \in \mathcal{X}_i$. According to KKT conditions, we have

$$0 \in f_{ix}(\pi_i(v)) + A_i^\top \lambda(v) + C_{\mathcal{X}_i}(\pi_i(v)), \tag{17}$$

$$\sum_{i=1}^{n} A_i \pi_i(v) = \sum_{i=1}^{n} B_i \left(r_i(v) + e_i\right). \tag{18}$$

where $C_{\mathcal{X}_i}(\pi_i(v))$ denotes the feasible direction cone.

While there is no analytical solution for time derivative of (17), we can view the projection operator as a quadratic activation function $p_i(x_i)$ with an infinitely large magnitude to penalize constraint violations. As a result, Problem (13) is equivalent to

$$\begin{aligned} \min_{x_i \in \mathbb{R}, \forall i} \max_{\lambda \in \mathbb{R}^2} & \sum_{i=1}^{n} f_i(x_i) + \sum_{i=1}^{n} p_i(x_i) \\ & + \sum_{i=1}^{n} \lambda^\top \left[A_i x_i - B_i \left(r_i(v) + e_i\right)\right]. \end{aligned} \tag{19}$$

Consider a binary function to signify whether the projection operator is activated or not

$$\delta_i(z) = \begin{cases} 0, & \text{if } \mathcal{P}_{\mathcal{X}_i}(z+\epsilon) = z, \forall \epsilon \in \mathbb{R}_{++}, \\ 1, & \text{else}, \end{cases} \tag{20}$$

where $\mathcal{P}_{\mathcal{X}_i}(z)$ represents the projection of a scalar z into a definition domain $\mathcal{X}_i$. By virtue of (19), the time derivatives of (17)–(18), except for the case where π_i is on the boundary and moving inward, can be equivalently expressed as

$$\left(f_{ixx} + p_{ixx}\right) \pi_{iv} Sv + A_i^\top \lambda_v Sv = 0, \tag{21}$$

$$\sum_{i=1}^{n} A_i \pi_{iv} Sv = \sum_{i=1}^{n} B_i \left(r_{iv} Sv + \frac{\partial e_i}{\partial t}\right), \tag{22}$$

where the subgradient of δ_i is chosen to be 0, $f_{ixx} = \frac{\partial f_i^2}{\partial^2 x_i} \in \mathbb{R}_{++}$, $p_{ixx} = \frac{\partial p_i^2}{\partial^2 x_i} \in \mathbb{R}_{+}$, $\lambda_v = \frac{\partial \lambda}{\partial v} \in \mathbb{R}^{(1+z)\times 2N}$, $\pi_{iv} = \frac{\partial \pi_i}{\partial v} \in \mathbb{R}^{1\times 2N}$, and $r_{iv} = \frac{\partial r_i}{\partial v} \in \mathbb{R}^{(1+z)\times 2N}$, which remains constant if the USTF profile is not updated.

Note that for the feedforward design, adopting (21) also for the special case, which lasts only for an infinitesimal neighborhood of that specific moment, will not affect the results since π_i will instantly move away from the boundary. As $\lim p_{ixx} \to \infty$ for $x_i \notin \mathcal{X}_i$ and $p_{ixx} = 0$ otherwise, it can be readily inferred from (21) that

$$\pi_{iv} = -\delta_i(\pi_i) f_{ixx}^{-1} A_i^\top \lambda_v. \tag{23}$$

To explicitly obtain π_{iv}, we need to obtain λ_v first. However, e_i in (22) manifests as a stochastic signal which cannot be exactly described nor predicted. Thus, it is not a kind of prior information we can utilize for the feedforward design. This underscores the importance of USTF profiles being able to reasonably depict the drift of demand, which is equivalent to assuming that e_i is time-invariant. In fact, for the notation of (16) we have implicitly introduced the following assumption:

Assumption 1: There is no direct dependence of e_i on time, i.e., its gradient or subgradient $\frac{\partial e_i}{\partial t} = 0$, $\forall i$.

This holds true when N is sufficiently large under the premise of the integrity of USTF profiles. Under Assumption 1, substituting (23) into (22) returns

$$\sum_{i=1}^{n} A_i \pi_{iv} = -\sum_{i=1}^{n} \delta_i(\pi_i) f_{ixx}^{-1} A_i A_i^\top \lambda_v = \sum_{i=1}^{n} B_i r_{iv}. \tag{24}$$

As a result, we can obtain the following criterion:

$$\lambda_v = -\left(\sum_{i=1}^{n} \delta_i(\pi_i) f_{ixx}^{-1} A_i A_i^\top\right)^\dagger \sum_{i=1}^{n} B_i r_{iv}. \tag{25}$$

Remark 2: This representation benefits from a coordinate transformation through the exosystem, where the drifts (with respect to the exosystem) of the time-varying optimal trajectories become time-invariant. This characteristic simplifies the analysis of the TVOP, as time-invariant problems are relatively well-understood. However, the validity of (23) and (25) is subject to the integrity of USTF profiles. In extreme cases, feedforward laws based on them may yield counterproductive control effects. Step load changes are inconsequential because they are time-invariant.

C. Distributed Auxiliary Protocol

It is worth noting that (25) involves a significant amount of global information that is not accessible in a distributed implementation. Regarding this, a distributed auxiliary protocol is developed, which involves each node communicating with its neighbors and updating its own estimate of λ_v based on the information it receives:

$$\dot{\xi}_i = -\sum_{j=1}^{n} l_{ij} \xi_j - \sum_{j=1}^{n} l_{ij} \eta_j - w_i \xi_i + B_i r_{iv}, \tag{26}$$

$$\dot{\eta}_i = \sum_{j=1}^{n} l_{ij} \xi_j, \tag{27}$$

where $\xi_i \in \mathbb{R}^{n(1+z)\times 2N}$, $\eta_i \in \mathbb{R}^{n(1+z)\times 2N}$, l_{ij} is the ijth entry of the Laplacian matrix, and $w_i \in \mathbb{R}^{(1+z)\times(1+z)}$ is a weighting matrix to be designed now.

By letting $\dot{\eta}_i = 0$, from (27) we know that the auxiliary protocol converges at: $\xi_i = \xi_j = \xi_0$ for all i, j, where ξ_0 is temporarily introduced to ease our derivations. Let $\dot{\xi}_i = 0$ and left-multiply (26) by $\mathbf{1}^\top$. We have $\sum_{i=1}^{n} w_i \xi_i = \sum_{i=1}^{n} w_i \xi_0 = \sum_{i=1}^{n} B_i r_{iv}$, which implies

$$\xi_0 = \left(\sum_{i=1}^{n} w_i\right)^\dagger \sum_{i=1}^{n} B_i r_{iv}. \tag{28}$$

Referring back to (25), ξ_i provides an estimate of $-\lambda_v$ if

$$w_i = \delta_i(x_i) f_{ixx}^{-1} A_i A_i^\top, \tag{29}$$

and ultimately we will have

$$\lambda_v = -\xi_i, \tag{30}$$

$$\pi_{iv} = \delta_i(\pi_i) f_{ixx}^{-1} A_i^\top \xi_i, \tag{31}$$

if both x_i and ξ_i converge to their desired values. However, the following assumptions are needed.

Assumption 2: 1) The Slater's condition holds; 2) the communication network is connected and undirected; 3) $f_i(x_i), \forall i$ are quadratic convex functions; 4) x_i can always converge to $\Omega_i = \{x_i \in \mathbb{R} : \delta_i(x_i) = \delta_i(\pi_i(v))\}$ for all i.

D. Distributed Optimization Algorithm

The idea of feedforward optimization is about including some extra terms to provide desired variations to x_i and λ_i, so that x_i and λ_i are enforced to track $\pi_i(v)$ and $\lambda(v)$ [17]. The desired variations for the primal and dual are

$$\dot{\pi}_i(v) = \pi_{iv} S v, \tag{32}$$

$$\dot{\lambda}(v) = \lambda_v S v. \tag{33}$$

By combining (30)–(33), we propose a projection-based distributed optimization algorithm as follows:

$$\dot{x}_i = \mathcal{P}_{\mathcal{X}_i}\left(x_i - f_{ix} - A_i^\top \lambda_i + \alpha_i\right) - x_i, \tag{34}$$

$$\begin{aligned}\dot{\lambda}_i = {} & A_i x_i - B_i d_i(t) - \sum_{j=1}^{n} l_{ij}\lambda_j - \sum_{j=1}^{n} l_{ij} z_j + \beta_i, \\ & + f_{ixx}^{-1} A_i \left(-A_i^\top \lambda_i - f_{ix}(0)\right) - B_i r_{iv},\end{aligned} \tag{35}$$

$$\dot{z}_i = \sum_{j=1}^{n} l_{ij}\lambda_j, \tag{36}$$

where α_i and β_i are feedforward laws given by

$$\alpha_i = \delta_i(x_i) f_{ixx}^{-1} A_i^\top \xi_i S v, \tag{37}$$

$$\beta_i = -\xi_i S v. \tag{38}$$

Theorem 1: For the dynamical system described by (26)–(27) and (34)–(36), under Assumptions 1 and 2, if the initial conditions are set as $\eta_i(0) = 0$ and $z_i(0) = 0$, $\forall i$, then its state x_i, $\forall i$, can asymptotically converge to the time-varying optimal trajectory for problem (13).

Proof: Due to limited space, we do not provide a detailed proof in this paper; instead, we present an outline to show the convergence and optimality. Denote $\tilde{\xi}_i$ and $\tilde{\eta}_i$ as the equilibrium points for (26)–(27), $\tilde{x}_i$, $\tilde{\lambda}_i$, and $\tilde{z}_i$ as the equilibrium points for (34)–(36). Construct a Lyapunov candidate $V = \frac{1}{2}\sum_{i=1}^{n}\left(\|\bar{x}_i\|^2 + \|\bar{\lambda}_i\|^2 + \|\bar{z}_i\|^2\right) + \frac{k}{2}\sum_{i=1}^{n}\left(\|\bar{\xi}_i\|^2 + \|\bar{\eta}_i\|^2\right)$, where $\bar{x}_i = x_i - \tilde{x}_i$, $\bar{\lambda}_i = \lambda_i - \tilde{\lambda}_i$, $\bar{z}_i = z_i - \tilde{z}_i$, $\bar{\xi}_i = \xi_i - \tilde{\xi}_i$, and $\bar{\eta}_i = \eta_i - \tilde{\eta}_i$, and $k \in \mathbb{R}_{++}$. The terms in the second row of (35) contribute to making $\dot{V}$ negative-definite. Invoking the properties of projection and quadratic convex functions, and from the boundness of v, one can ultimately derive $\dot{V} \leq 0$ provided a sufficiently big k. Proof on asymptotic convergence is complete by LaSalle's invariance principle. Then one can easily prove the equivalence of equilibrium points and optimal solution. ■

V. Case Studies

This section aims to demonstrate the effectiveness of the proposed scheme through a simulation study on a 5-node MEN. We configure a single thermal zone, with all three load buses (Node 2, Node 3, and Node 4) enclosed and consider their collective responsibility in meeting $\dot{Q}_{1,L}(t)$. The responses of central plant and WSHPs are modeled by single-integrator or double-integrator dynamics. We consider constant mass flow rate at the central plant, with the supply water temperature fluctuating around 20 °C. On the user side, it is set that $T_{i,u} = 40$ °C. The layout of the test network is shown in Fig. 3, including both physical network and communication network. The communication network topology can be rather flexible as long as a direct spanning tree is ensured. The modeling parameters are selected from [22], and the profiles are obtained from the Pecan Street dataset [28]. The least square method is adopted for processing the USTF profiles with a time resolution of 10 s, and we use $N = 5$. Therefore, $v \in \mathbb{R}^{10}$ and $S \in \mathbb{R}^{10\times 10}$. For practical implementation, (26)–(27) and (34)–(36) have been discretized with a control interval of 0.1 s.

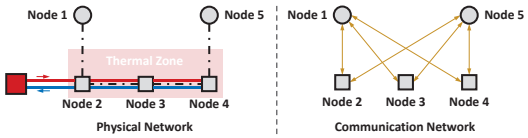

Fig. 3. Test MEN with 5 nodes and 1 thermal zone.

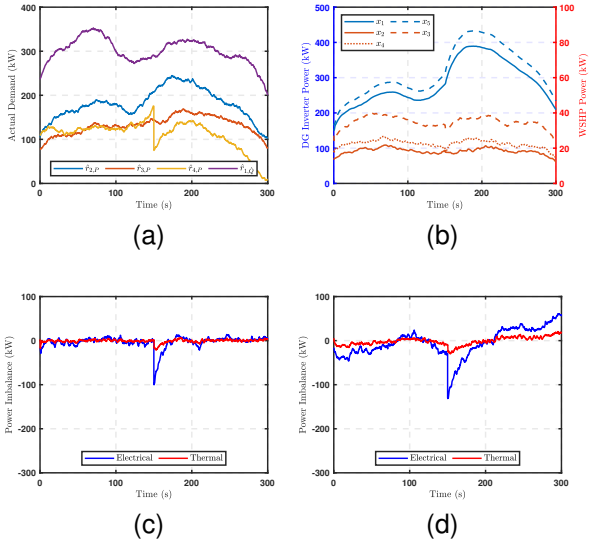

Fig. 4. Simulation results under the presence of real-world errors: (a) actual demands; (b) optimized power set points; (c) real-time power imbalances with the proposed scheme; (d) real-time power imbalances with [7].

Simulation is carried out under the presence of real-world errors, which are emulated by introducing uncertainties to r_{iv} as well as some noisy signals, as depicted in Fig. 4(a). In addition, an 100 kW step increase in electrical power demand is introduced to Node 4 at 150 s. Concerning network stability, the initial states are reasonably configured and the simulation results are given in Figs. 4(b)–(c), where sub-figure (b) shows the optimized power set points and sub-figure (c) gives the real-time power imbalances. The dispatchable units exhibit different responses due to their

inherent heterogeneity in cost functions. Overall, although some slight violations of equality constraint, reflected as real-time power imbalance, may occur, our proposed scheme provides satisfactory tracking performance in such a non-ideal case.

The performance of the proposed scheme is compared with a distributed ORA algorithm modified from [7], which is purely feedback-based and lacks of feedforward laws to cancel the effects of temporal variations. By comparing Figs. 4(c)–(d), it can be concluded that feedforward optimization possesses superior performance especially in a highly variable environment, as [7] always exhibits significant power imbalances. At 150 s, when an unforeseen load increase occurs, significant power deficiencies can be observed for both electrical and thermal, indicating a coupling effect between the two. The deficiencies are more pronounced in Fig. 4(d) due to the lack of a feedforward design. A quantitative comparison between Figs. 4(c)–(d) is also provided to show the significantly improved performance. For the time window starting at 200 s and ending at 300 s, the Root Mean Square Errors (RMSEs) for our scheme and [7] are respectively 5.80/2.33 and 31.89/9.40 kW (electrical/thermal). We would like to highlight that the performance of the proposed scheme is subject to the integrity of USTF profiles, and under ideal case, it can attain zero tracking error, fully canceling out the effects of temporal variations.

VI. Conclusion

This paper has studied a distributed TVOP for control of MEN. By revisiting some previous findings, we have developed a fully distributed optimization scheme that incorporates a feedforward design and a data-driven feature. Local feasibility constraints have been strictly handled using projection, different from the existing results. Analyses and simulation results have demonstrated the effectiveness of the proposed scheme under realistic conditions. Ideally, it can follow the optimal trajectory with tracking error asymptotically converging to zero. As future work, the proposed scheme needs to be validated on MENs with a realistic size.

References

[1] S. Pye, F. G. Li, J. Price, and B. Fais, "Achieving net-zero emissions through the reframing of UK national targets in the post-paris agreement era," *Nat. Energy*, vol. 2, no. 3, pp. 1–7, 2017.

[2] E. Guelpa, A. Bischi, V. Verda, M. Chertkov, and H. Lund, "Towards future infrastructures for sustainable multi-energy systems: A review," *Energy*, vol. 184, pp. 2–21, 2019.

[3] K. Gjoka, B. Rismanchi, and R. H. Crawford, "Fifth-generation district heating and cooling systems: A review of recent advancements and implementation barriers," *Renew. Sust. Energ. Rev.*, vol. 171, p. 112997, 2023.

[4] F. Bünning, M. Wetter, M. Fuchs, and D. Müller, "Bidirectional low temperature district energy systems with agent-based control: Performance comparison and operation optimization," *Appl. Energy*, vol. 209, pp. 502–515, 2018.

[5] L. M. P. Ghilardi, A. F. Castelli, L. Moretti, M. Morini, and E. Martelli, "Co-optimization of multi-energy system operation, district heating/cooling network and thermal comfort management for buildings," *Appl. Energy*, vol. 302, p. 117480, 2021.

[6] M. Taylor, S. Long, O. Marjanovic, and A. Parisio, "Model predictive control of smart districts with fifth generation heating and cooling networks," *IEEE Trans. Energy Convers.*, vol. 36, no. 4, pp. 2659–2669, 2021.

[7] P. Yi, Y. Hong, and F. Liu, "Initialization-free distributed algorithms for optimal resource allocation with feasibility constraints and application to economic dispatch of power systems," *Automatica*, vol. 74, pp. 259–269, 2016.

[8] S. Rahili and W. Ren, "Distributed continuous-time convex optimization with time-varying cost functions," *IEEE Trans. Automat. Control*, vol. 62, no. 4, pp. 1590–1605, 2016.

[9] C. Sun, M. Ye, and G. Hu, "Distributed time-varying quadratic optimization for multiple agents under undirected graphs," *IEEE Trans. Automat. Control*, vol. 62, no. 7, pp. 3687–3694, 2017.

[10] M. Fazlyab, S. Paternain, V. M. Preciado, and A. Ribeiro, "Prediction-correction interior-point method for time-varying convex optimization," *IEEE Trans. Automat. Control*, vol. 63, no. 7, pp. 1973–1986, 2017.

[11] A. Simonetto and E. Dall'Anese, "Prediction-correction algorithms for time-varying constrained optimization," *IEEE Trans. Signal Process.*, vol. 65, no. 20, pp. 5481–5494, 2017.

[12] A. Simonetto, A. Koppel, A. Mokhtari, G. Leus, and A. Ribeiro, "Decentralized prediction-correction methods for networked time-varying convex optimization," *IEEE Trans. Automat. Control*, vol. 62, no. 11, pp. 5724–5738, 2017.

[13] B. Wang, Q. Fei, and Q. Wu, "Distributed time-varying resource allocation optimization based on finite-time consensus approach," *IEEE Control Syst. Lett.*, vol. 5, no. 2, pp. 599–604, 2020.

[14] B. Wang, S. Sun, and W. Ren, "Distributed continuous-time algorithms for optimal resource allocation with time-varying quadratic cost functions," *IEEE Trans. Control. Netw. Syst.*, vol. 7, no. 4, pp. 1974–1984, 2020.

[15] B. Wang, S. Sun, and W. Ren, "Distributed time-varying quadratic optimal resource allocation subject to nonidentical time-varying hessians with application to multiquadrotor hose transportation," *IEEE Trans. Syst. Man Cybern.: Syst.*, vol. 52, no. 10, pp. 6109–6119, 2022.

[16] C. Wu, H. Fang, X. Zeng, Q. Yang, Y. Wei, and J. Chen, "Distributed continuous-time algorithm for time-varying optimization with affine formation constraints," *IEEE Trans. Automat. Control*, vol. 68, no. 4, pp. 2615–2622, 2023.

[17] Z. Ding, "Distributed time-varying optimization—an output regulation approach," *IEEE Trans. Cybern.*, 2022.

[18] M. Tan, S. Yuan, S. Li, Y. Su, H. Li, and F. He, "Ultra-short-term industrial power demand forecasting using lstm based hybrid ensemble learning," *IEEE Trans. Power Syst.*, vol. 35, no. 4, pp. 2937–2948, 2019.

[19] C. Tong, L. Zhang, H. Li, and Y. Ding, "Temporal inception convolutional network based on multi-head attention for ultra-short-term load forecasting," *IET Gener. Transm. Distrib.*, vol. 16, no. 8, pp. 1680–1696, 2022.

[20] M. Bilardo, F. Sandrone, G. Zanzottera, and E. Fabrizio, "Modelling a fifth-generation bidirectional low temperature district heating and cooling (5GDHC) network for nearly zero energy district (nZED)," *Energy Rep.*, vol. 7, pp. 8390–8405, 2021.

[21] F. Dörfler, J. W. Simpson-Porco, and F. Bullo, "Breaking the hierarchy: Distributed control and economic optimality in microgrids," *IEEE Trans. Control Netw. Syst.*, vol. 3, no. 3, pp. 241–253, 2015.

[22] X. Liu, J. Wu, N. Jenkins, and A. Bagdanavicius, "Combined analysis of electricity and heat networks," *Appl. Energy*, vol. 162, pp. 1238–1250, 2016.

[23] X. Xu, Q. Lyu, M. Qadrdan, and J. Wu, "Quantification of flexibility of a district heating system for the power grid," *IEEE Trans. Sustain. Energy*, vol. 11, no. 4, pp. 2617–2630, 2020.

[24] Z. Li, W. Wu, M. Shahidehpour, J. Wang, and B. Zhang, "Combined heat and power dispatch considering pipeline energy storage of district heating network," *IEEE Trans. Sustain. Energy*, vol. 7, no. 1, pp. 12–22, 2015.

[25] E. A. M. Cesena, E. Loukarakis, N. Good, and P. Mancarella, "Integrated electricity–heat–gas systems: Techno–economic modeling, optimization, and application to multienergy districts," *Proc. IEEE*, vol. 108, no. 9, pp. 1392–1410, 2020.

[26] Y. Xu, Z. Dong, Z. Li, Y. Liu, and Z. Ding, "Distributed optimization for integrated frequency regulation and economic dispatch in microgrids," *IEEE Trans. Smart Grid*, vol. 12, no. 6, pp. 4595–4606, 2021.

[27] B. A. Francis and W. M. Wonham, "The internal model principle of control theory," *Automatica*, vol. 12, no. 5, pp. 457–465, 1976.

[28] Pecan Street Inc., "Pecan street dataport," 2019. https://www.pecanstreet.org/dataport [online].